J. Synchrotron Rad. (1998). **5**, 980–982

X-ray parametric scattering by a diamond crystal

Y. Yoda,[a]* T. Suzuki,[a] X.-W. Zhang,[b] K. Hirano[b] and S. Kikuta[a]

[a]Department of Applied Physics, School of Engineering, University of Tokyo, 7-3-1 Hongo, Bunkyo-ku, Tokyo 113, Japan, and [b]Photon Factory, High Energy Accelerator Research Organization, 1-1 Oho, Tsukuba-shi, Ibaraki 305, Japan. E-mail: yoda@kohsai.t.u-tokyo.ac.jp

(*Received 4 August 1997; accepted 23 December 1997*)

Spontaneous X-ray parametric scattering from a diamond single crystal has been observed at the Photon Factory. The high perfection of the diamond single crystal and the small angular divergence of synchrotron radiation has enabled down-converted X-ray photon pairs to scatter into two small solid angles which satisfy the phase-matching condition. High-efficiency noise reduction was performed using avalanche photodiode detectors with good time resolution.

Keywords: X-ray parametric scattering; non-linear effect; diamond; avalanche photodiode detectors; phase matching.

1. Introduction

One X-ray photon of the angular frequency ω_p is converted into two photons of ω_1 and ω_2 conserving its energy ($\omega_p = \omega_1 + \omega_2$) in the spontaneous X-ray parametric down-conversion process. This phenomenon is understood as the non-linear effect of the incident photon coupling with the zero-point fluctuation of the vacuum field and was first observed by Eisenberger & McCall (1971). In their work Mo $K\alpha$ radiation from an X-ray tube was incident on a beryllium single crystal and coincident photon pairs were observed with two scintillation detectors. Although edge enhancement (Kleinman, 1968) was employed, it was difficult to use the emitted photons as an exploring beam for X-ray optics experiments. This was because the solid angle of the emitted photons was not small enough on account of the wide angular divergence of the incident X-ray and the imperfection of the beryllium crystal.

Because the resonance decreases the interaction strength (Freund & Levine, 1969) and heavier material absorbs the emitted photon more strongly, a crystal composed of light atoms is considered more suitable in general for the analysis of the parametric down conversion. Diamond is one of the most attractive crystals, as pointed out by Freund & Levine (1969). The latest advances in the perfection of diamond crystals (Sumiya *et al.*, 1997) and the brilliance of synchrotron radiation make it possible for the down-converted X-ray photon pairs to be emitted into a small solid angle, even in the same direction in the special case.

2. Phase-matching condition

The down-converted photon pairs are strongly emitted in the direction that satisfies the energy conservation and the phase-matching condition in which the X-rays are scattered in phase. In the crystal, the reciprocal lattice vector can be utilized for the phase-matching condition as shown in Fig. 1 and is given by

$$\mathbf{k}_p + \mathbf{G} = \mathbf{k}_1 + \mathbf{k}_2, \tag{1}$$

where $\mathbf{k}_p$, $\mathbf{k}_1$, $\mathbf{k}_2$ are the wavevectors in the crystal and $\mathbf{G}$ is one of the reciprocal lattice vectors. When $\mathbf{k}_1$ is parallel to $\mathbf{k}_2$, the X-ray photons are emitted in the same direction. The rotation angle of the crystal in this condition is slightly different from the Bragg angle owing to the difference in the refractive indices of $\mathbf{k}_p$ and $\mathbf{k}_1$ ($\mathbf{k}_2$). In the case of $|\mathbf{k}_1| \simeq |\mathbf{k}_2|$, the deviation angle $\delta\theta_n$ has the form

$$\delta\theta_n = (n_p - n_1)/\sin 2\theta_B, \tag{2}$$

where n_p and n_1 are the refractive indices and θ_B is the Bragg angle. The angle between $\mathbf{k}_p + \mathbf{G}$ and $\mathbf{k}_1$ is expressed as (Eisenberger & McCall, 1971)

$$R(x) = [2(\delta\theta_B - \delta\theta_n)(y/x)\sin 2\theta_B]^{1/2} \tag{3}$$

where $\delta\theta_B$ is the rotation angle from the Bragg angle and x and y are defined by $\omega_1 = x\omega_p$ and $\omega_2 = y\omega_p$. If $(\delta\theta_B - \delta\theta_n)$ is negative, this equation is not effective or the phase-matching condition is not satisfied for any direction of $\mathbf{k}_1$, $\mathbf{k}_2$. The cross section of the parametric scattering is written in the form (Freund & Levine, 1969)

$$\mathrm{d}\sigma/\mathrm{d}\Omega \propto [R(x) + R(y)]^{-2}. \tag{4}$$

As is evident from (3) and (4), it is essential to make $(\delta\theta_B - \delta\theta_n)$ as small as possible so that the X-ray photons are emitted in a small solid angle.

3. Experimental

The experiment was performed at the vertical wiggler beamline BL-14B (Ando *et al.*, 1986) of the Photon Factory (KEK). The storage ring was operated in multi-bunch mode with a 2 ns pulse interval. X-rays of wavelength 0.65 Å from an Si 111 double-crystal monochromator were incident on a diamond single crystal as shown in Fig. 2. Symmetric Bragg case 400 and 111 reflections of diamond were employed for the phase matching. The sizes of (400) and (111) crystal plates were 4 × 4 × 0.5 and 3.5 × 5.5 × 0.6 mm, respectively. The incident X-ray beam was restricted by X–Y slits to 3 (v) × 1 (h) mm for 400 reflection and 3 (v) × 0.8 (h) mm for 111 reflection, and the incident fluxes measured by the PIN detector were 2.5×10^9 and 2.1×10^9 counts s^{-1}, respectively, at a ring current of 300 mA. An angular divergence of the incident X-rays calculated from the source size and the slit size was

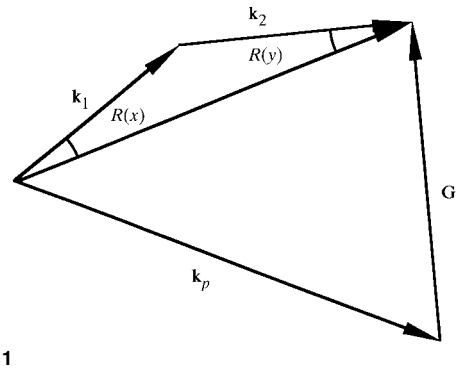

Figure 1
The phase-matching condition of the parametric scattering. $\mathbf{k}_p$: wavevector of the incident X-ray, $\mathbf{G}$: reciprocal lattice vector, $\mathbf{k}_1$, $\mathbf{k}_2$: wave-vectors of the down-converted X-rays. The refractive index for X-rays is so close to unity that the locus of $\mathbf{k}_1$ makes nearly an ellipsoid of revolution.

approximately 0.2 (v) × 0.1 (h) mrad. The horizontal divergence leads to $\Delta E/E = 1 \times 10^{-3}$ from the relation $\Delta E/E = \Delta\theta/\tan\theta_B$ (ignoring the intrinsic width), which was also confirmed experimentally by the width of the rocking curve from a non-parallel setting of Si 111 and diamond 400 reflections. The diamond crystal was attached to the sample holder, which was designed to allow a direct beam to pass through for the purpose of reducing the background noise. It was mounted on the vertical axis high-precision diffractometer with a finest step of 0.005 arcsec.

Two avalanche photodiode (APD) detectors (Kishimoto, 1992), 5 mm square with their centers separated by 18 mm, were placed on the scattering plane so as to be symmetric about the direction of the Bragg reflection. The distance between the diamond crystal and the APD detectors was 350 mm for the 400 reflection and 1135 mm for the 111 reflection.

The combination of the energy analysis and coincidence technique was used as in previous work (Eisenberger & McCall, 1971) to reduce the background noise mainly coming from Thomson scattering and Compton scattering. In our study, the APD detectors were used in the place of the NaI–Th scintillation detectors. The energy resolution of the APD detectors was approximately 50% with an asymmetric shape, as a result of analysis using the differential constant fractional discriminator (CFD), and the time resolution was 0.46 ns. The quantum efficiency was 60% for the 1.3 Å X-rays and 12% for the 0.65 Å X-rays. The lower and upper levels of the differential CFD were determined so that the 1.3 Å X-rays came to the center of the selected range and the background noise became sufficiently low. The coincidence unit passed the signal when X-ray photons were detected by both detectors in the same bunch, that is, at about 1.5 ns coincidence width. The fine adjustment of the simultaneity of the two electronic circuits was performed by changing the cable length.

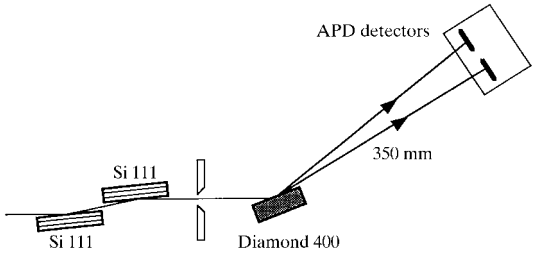

Figure 2
Schematic experimental set-up. Two APD detectors were arranged. The 111 reflection of diamond was also used instead of the 400 reflection.

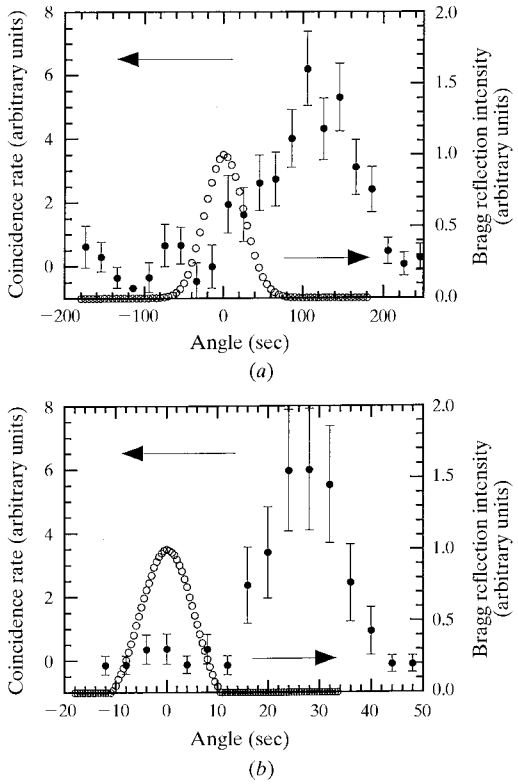

Figure 3
Angular scan of the diamond crystal (*a*) for 400 reflection and (*b*) for 111 reflection. Black circles: coincidence rate of two APD detectors. White circles: Bragg reflection intensity detected by one APD detector placed on the Bragg reflection direction.

4. Results and discussion

The coincidence signal was measured by rotating the diamond crystals step by step. The coincidence rate with the subtraction of the accidental coincidence rate from the measured signal is plotted as black circles in Fig. 3(*a*) for the 400 reflection and Fig. 3(*b*) for the 111 reflection. The Bragg reflection intensities are also plotted as white circles. The coincidence peaks are clearly seen at the higher angle side of the Bragg reflection peak and the signals at the peaks were 6 counts h^{-1} in both reflections. The subtracted accidental coincidence rates, which can be calculated from the counts measured by each detector, are 2.7 counts h^{-1} at most for the 400 reflection and 0.2 counts h^{-1} at most for the 111 reflection. The accidental coincidence for the 400 reflection mainly comes from the scattering of the Bragg reflected beam from the detector window and so it is less than 0.5 counts h^{-1} outside the Bragg reflection region. The lower background noise level was achieved by shielding the Bragg reflected beam for the 111 reflection.

At the peak of the coincidence rate for the 111 reflection, the change of the coincidence rate was measured by adjusting the delay cable. As shown in Fig. 4, in the case where the delay time is more than 1.5 ns no signal is counted. This means that the peak of the coincidence rate for the 111 reflection is certainly formed by the simultaneous detection by the two detectors. The expected

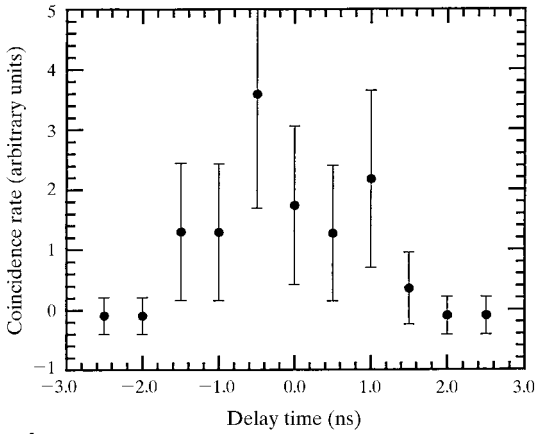

Figure 4
Intensity profile observed by changing the coincidence timing by means of the delay cable. This profile was measured at the peak of the coincidence rate curve for 111 reflection.

peak profile of the coincidence rate without the energy dispersion can be numerically calculated from (3) and (4) assuming $x \simeq y$. Here the accepted region of $R(x)$ is determined by the detector's area and the angle from $6.5/L$ to $11.8/L$ is assumed to be uniformly effective where L (mm) is the distance between the diamond crystal and the APD detectors. For the 400 reflection the calculated angular position of its peak is 96 s, deviated to the high-angle side of the Bragg reflection and including the shift of 1.7 s due to the effect of refraction, and its width is 56 s. For the 111 reflection the calculated angular position of its peak is 24.4 s including the shift of 3.9 s due to the effect of refraction, and its width is 11.8 s. In any case X-ray photons whose energies are about 40–60% of the incident photon's energy are detected simultaneously because of the arrangement of the detectors. The measured profile is broadened in width by the convolution with the Bragg reflection profile, which mainly comes from the non-parallel arrangement between the Si reflection and the diamond reflection. Except for the width of the 111 reflection, there is a discrepancy in the peak angle and its width between the measured profile and the expected one. The measured peak angle shifts slightly to the higher angle. However, taking into account the approximations used in the calculation, the measured profile agrees fairly well with the expected one. In the calculation, $x \simeq y$ is assumed and many factors are ignored, such as the energy dependence of the quantum efficiency of the APD, the energy dependence of the absorption by the crystal and the air, the detector's shape and the incident beam size. For detailed analysis, more accurate calculation may be needed in addition to the reduction of the statistical error of the data. The effect of the refraction is clearly seen in the 111 reflection because when it is neglected the expected peak angle is 20.5 s, which is far away from the measured peak.

Following the count-rate equation (Levine & Freund, 1970) and applying the same approximation described above, 120 counts h^{-1} for the 400 reflection and 44 counts h^{-1} for the 111 reflection are estimated. In our arrangement the dephasing in the unit cell for the 111 reflection and the polarization factor of $8\sin^2 2\theta_B$ were taken into account. The difference from the measured count rate of 6 counts h^{-1} is mainly attributed to the low quantum efficiency of the APD. The reason why the measured rates are the same in the 400 reflection and the 111 reflection in spite of the difference in the expected rates may be the smaller energy range of the discriminator for the 400 reflection compared with that for the 111 reflection, adjusted to decrease the accidental coincidence.

5. Summary

Spontaneous X-ray parametric scattering from the diamond single crystal has been observed. The high perfection of the diamond single crystal and the small angular divergence of synchrotron radiation enabled parametric scattering to be detected near the Bragg angle. The converted photon pairs were scattered into two small solid angles, which suggests the possibility of the detailed analysis of the parametric scattering like the polarization analysis. The good time resolution of the APD detector and the small solid angle of the emitted down-converted photons made it possible to reduce the noise efficiently.

The authors acknowledge Dr Sumiya (Sumitomo Electric Industries Ltd) for the loan of the diamond crystal. This work was partially supported by a Grant-in-Aid from the Ministry of Education, Science, Sports and Culture.

References

Ando, M., Satow, Y., Kawata, H., Ishikawa, T., Spieker, P. & Suzuki, S. (1986). *Nucl. Instrum. Methods A*, **246**, 144–148.
Eisenberger, P. & McCall, S. L. (1971). *Phys. Rev. Lett.* **26**, 684–688.
Freund, L. & Levine, B. F. (1969). *Phys. Rev. Lett.* **23**, 854–857.
Freund, L. & Levine, B. F. (1971). *Opt. Commun.* **3**, 101–104.
Kishimoto, S. (1992). *Nucl. Instrum. Methods A*, **309**, 603–605.
Kleinman, D. A. (1968) *Phys. Rev.* **174**, 1027–1041.
Levine, B. F. & Freund, L. (1970). *Opt. Commun.* **1**, 419–422.
Sumiya, H., Toda, N., Nishibayashi, Y. & Satoh, S. (1997) *J. Cryst. Growth*, **178**, 485–494.